

## **Building Footprint Extraction from LiDAR Data Using SVM Classification**

V.Vakula, P.Anitha, C.Sasikala

### **Abstract**

Automatic detection of buildings from very high resolution (VHR) satellite images is a current research hotspot in remote sensing. In this work presents a novel approach to detect the buildings by atomization of the training area collecting stage for supervised classification. The classification method for the analysis of satellite image based on Normalized Difference Vegetation Index (NDVI). The method employs the multi-spectral remote sensing data technique to find spectral signature of different objects such as vegetation index, land cover classification, concrete structure, road structure, rural and urban areas, rocky areas and remaining areas presented in the image. In the experiments, the proposed SVM framework outperformed for the three (Linear SVM, Cubic SVM, Medium Gaussian SVM) methods tested. SVM is trained through supervised learning to classify each location in the image as “buildings” or “Non-buildings.” Finally, SVM algorithm to find the accuracy value, training time and receiver operating characteristic curves to evaluate detection performance, and compare the proposed algorithm with several existing methods.

### **INTRODUCTION:**

The remote sensing information has numerous application areas including land cover classification, soil moisture measurement, and forest type classification, estimation of the fluid water substance of vegetation, snow mapping, ocean ice type characterization, and oceanography. The multispectral remote sensing images carries essential integrating spectral and spatial features of the objects. It is extremely productive for acquiring a superior comprehension of the earth environment. It is the science and craft of gaining data and separating the highlights in the type of otherworldly, spatial and temporal about certain objects, area or phenomenon. For example vegetation, land cover classification, urban area, agriculture land, and water resources without coming into physical contact of these items. In this paper, the multispectral picture of Erode district is utilized to ascertain the level of flexible highlights, for example vegetation, water bodies, land spread arrangement, solid structures, rough zone, urban regions, street structure, and remaining zone exhibited in this image.

The Indian remote sensing agency uses two generic sensors that are working for the collection of information named passive remote sensing and active remote sensing. The passive remote sensing through a sun source of energy is used for gathering the satellite information. It contains an array of small sensors or detectors. It's used to record the amount of electromagnetic radiation that is reflected or emitted from the Earth's surface. The active remote sensing propagates its own electro-magnetic radiation and measures the return signal for the intensity level. Passive remote sensing is applied to the feature extraction and the active remote sensing is used for the radar imaging system.

The National Aeronautics and Space Administration (NASA) of USA collects a 7- band data that are used to the feature extraction. It is known as the Land Remote Sensing Satellite (LANDSAT) image. National Remote Sensing Agency collects the multispectral remote sensing data image of various region places and it is called the Indian National Satellite System (INSAT) image. The INSAT image consist 3-band data and the information is accomplished by the help of these 3 bands named near infrared band, red band and green band. Each band contains some specific information and with the help of these three bands, the features are extracted.

On the basis of wavelength, remote sensing is classified into three types as: visible and reflective infrared remote sensing, thermal infrared remote sensing, and microwave remote sensing. The visible red and near-infrared (NIR) bands of an INSAT image are used to identify areas containing significant vegetation and other different features (Buildings, Roads, Water areas, etc...).

The classification method is used to classify the different features of the remote sensing images. There are lots of learning algorithms for classification, for example, SVM, random forest, and neural network. In this work used to the SVM classification method. SVM classifier is a nonlinear method and the algorithm can perform is highly related to the input feature. The input feature is a representation that captures the essence of the object under classification. SVM is trained through supervised learning to classify each location in the image as “buildings” or “Non-buildings.” Finally, SVM algorithm to find the accuracy value, training time and roc characteristics. In this work, the study area is described in Section II. The proposed methodology of building detection and classification is described in Section III. Section IV contains the implementation results of the proposed method and the result discussions. Finally, conclusion is provided in Section V.

## Study Area

The Sathyamangalam (Rural area) of Tamilnadu is located between 10°29'15" to 11°43'11" N latitude and 76°50'46" to 77°27'22" E longitude covers 1400 km<sup>2</sup> The topography of the reserve is highly variable with plains, slopes, hills, streams and rivers. The current study is limited within the core zone area of the sathyamangalam (2272 sq.km), but this rural area is characterized by population density and buildings. This remote sensing project will start with the from google maps imagery a small region of Sathyamangalam. The current study area take two type of input images.



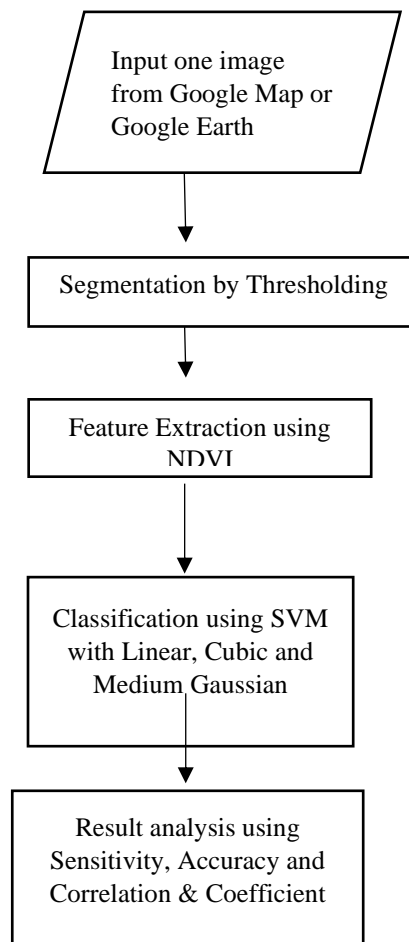
Figure (1): Input image of location (1a)



Figure (2): Input image of location (1b)

### Methodology:

#### System Architecture:



### Otsu's Image Segmentation Method:

Otsu's method is used to perform automatic image thresholding. In the simplest form, the algorithm returns a single intensity threshold that separate pixels into two classes, foreground and background. This threshold is determined by minimizing intra-class intensity variance, or equivalently, by maximizing inter-class variance.

The algorithm exhaustively searches for the threshold that minimizes the intra-class variance, defined as a weighted sum of variances of the two classes:

$$\sigma_w^2(t) = \omega_0(t)\sigma_0^2(t) + \omega_1(t)\sigma_1^2(t)$$

Weights  $\omega_0$  and  $\omega_1$  are the probabilities of the two classes separated by a threshold  $t$ ,  $\sigma_0^2$  and  $\sigma_1^2$  are variances of these two classes.

The class probability  $\omega_{0,1}(t)$  is computed from the  $L$  bins of the histogram:

$$\begin{aligned}\omega_0(t) &= \sum_{i=0}^{t-1} p(i) \\ \omega_1(t) &= \sum_{i=t}^{L-1} p(i)\end{aligned}$$

For 2 classes, minimizing the intra-class variance is equivalent to maximizing inter-class variance:

$$\begin{aligned}\sigma_b^2(t) &= \sigma^2 - \sigma_w^2(t) = \omega_0(\mu_0 - \mu_T)^2 + \omega_1(\mu_1 - \mu_T)^2 \\ &= \omega_0(t)\omega_1(t)[\mu_0(t) - \mu_1(t)]^2\end{aligned}$$

Which is expressed in terms of class probabilities  $\omega$  and class means  $\mu$ ,  $\mu_0(t)$ ,  $\mu_1(t)$  and  $\mu_T$  are:

$$\begin{aligned}\mu_0(t) &= \frac{\sum_{i=0}^{t-1} ip(i)}{\omega_0(t)} \\ \mu_1(t) &= \frac{\sum_{i=t}^{L-1} ip(i)}{\omega_1(t)} \\ \mu_T &= \sum_{i=0}^{L-1} ip(i)\end{aligned}$$

The following relations can be easily verified:

$$\begin{aligned}\omega_0\mu_0 + \omega_1\mu_1 &= \mu_T \\ \omega_0 + \omega_1 &= 1\end{aligned}$$

The class probabilities and class means can be computed iteratively. This idea yields an effective algorithm. And if the variances of the object and the background intensities are large compared to the mean difference, or

the image is severely corrupted by additive noise, the sharp valley of the gray level histogram is degraded. Then the possibly incorrect threshold determined by Otsu's method results in the segmentation error. Empirical results show that the performance of global thresholding techniques used for object segmentation (including Otsu's method) are limited by small object size, the small mean difference between foreground and background pixels, large variances of the pixels that belong to the object and those that belong to the background, the large amount of noise, etc.

At each pixel, the average gray-level value of the neighborhood is calculated. Let the gray level of the given pixel be divided into  $L$  discrete values and the average gray level is also divided into the same  $L$  values. Then a pair is formed: the pixel gray level and the average of the neighborhood  $(i, j)$ . Each pair belongs to one of the  $L \times L$  possible 2-dimensional bins. The total number of occurrences (frequency),  $f_{ij}$ , of a pair  $(i, j)$ , divided by the total number of pixels in the image  $N$ , defines the joint probability mass function in a 2-dimensional histogram:

$$P_{ij} = \frac{f_{ij}}{N}, \quad \sum_{i=0}^{L-1} \sum_{j=0}^{L-1} P_{ij} = 1$$

And the 2-dimensional Otsu's method is developed based on the 2-dimensional histogram as follows.

The probabilities of two classes can be denoted as:

$$\omega_0 = \sum_{i=0}^{s-1} \sum_{j=0}^{t-1} P_{ij}$$

$$\omega_1 = \sum_{i=s}^{L-1} \sum_{j=t}^{L-1} P_{ij}$$

### Features Extracting:

The Normalized Difference Vegetation Index (NDVI) procedure is utilized for separating the different highlights introduced in the 3-band satellite image of the segmentation area in the image. The 3-band data and the information is practiced by the assistance of these 3 bands named near-infrared band, red band and green band. Each band contains some particular data and with the assistance of these three bands, the features can be extracted. NDVI is determined as a ratio distinction between estimated overhang reflectance in the red and near-infrared bands individually. NDVI calculation shows the contrasts between the visible red and near-infrared (NIR) bands of an INSAT image can be utilized to distinguish regions containing critical vegetation and other various features.



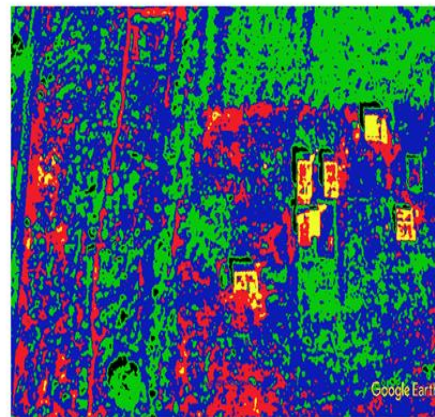
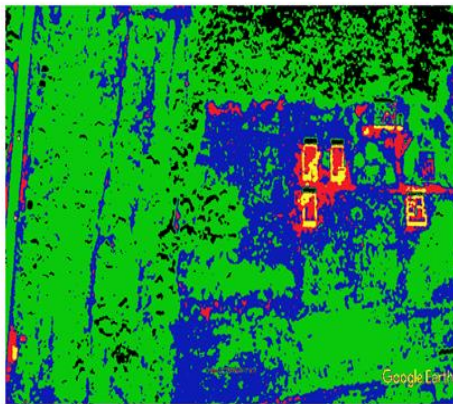
The NDVI is calculated as

$$RNDVI = \frac{NIR - RED}{NIR + RED} \quad (\text{where } 0 < NDVI < 1)$$

$$GNDVI = \frac{NIR - GREEN}{NIR + GREEN} \quad (\text{where } 0 < NDVI < 1)$$

where RED is visible red reflectance, and NIR is near-infrared reflectance. The wavelength scope of the NIR band is (750-1300 nm), Red band is (600-700 nm), and the Green band is (550 nm).

NDVI calculation, on a pixel by pixel premise subtracts the estimation of the red band from the estimation of the NIR band and partitions by their total, for example, shadows of buildings are removed. The extremely low estimation of NDVI (0.1 and underneath) relate to areas of rock, sand, or snow. Moderate esteems speak to bush and meadow (0.2 to 0.3), while high value indicates temperate (0.6 to 0.8). Exposed soil is spoken to with NDVI values, which are nearest to 0 and water bodies are spoken to with negative NDVI values. NDVI calculation to find a vegetation areas and to detect the another objects such as building shapes, roads and waste lands....etc,



Figure(3): Segmented output image of location (1a)    Figure(4): Segmented output image of location (2a)



Figure (4): Object identified location(1a)



Figure (5): Object identified location(2a)

### Support Vector Machine:

In this work the dataset consists of 100 aerial images of urban settlements in the Tamil Nadu and is labeled as building and non-building classes. Every image in the dataset is RGB and has 1568×1568 pixels resolution where each pixel corresponds to a 3cm×3cm of Earth surface. The high-resolution images of earth surfaces is sliced the image into multiple small resolution (256×256) images with some pixels of overlap. These sliced images are used to train the model. So for an image, 100 sliced are generated and the information about the location of the sliced image gets retained.

In this work Linear SVM, Cubic SVM and Medium Gaussian SVM are consider for classification. SVM is trained through supervised learning to classify each location in the image as “buildings” or “Non-buildings”. One method of Linear SVM is the newest extremely fast machine learning (data mining) algorithm for solving multiclass classification problems from ultra large data sets. The implements an original proprietary version of a cutting plane algorithm for designing a linear support vector machine. Linear SVM equation can be modified as follows:

$$J(\mathbf{w}, \xi) = \frac{1}{2} \|\mathbf{w}\|^2 + C \sum_{i=1}^l \xi_i$$

Where C is a user-specified, positive, regularization parameter. In  $\xi$  the variable is a vector containing all the slack variables  $\xi_i, i= 1, 2, \dots, l$ .

The regularization parameter C controls the trade-off. The purpose of using model complexity to constrain the optimization of empirical risk is to avoid overfitting, a situation in which the decision boundary too precisely corresponds to the training data, and thereby fails to perform well on data outside the training set. Linear SVM is a linearly scalable routine meaning that it creates an SVM model in a CPU time which scales linearly with

the size of the training data set. Our comparisons with other known SVM models clearly show its superior performance when high accuracy is required.

Explain to another method of Cubic SVM, classification is useful when a dilemma of low memory space is faced. SVM finds a hyperplane in multidimensional space which divides the classes into best possible way. Here cubic SVM type classifier is employed where the kernel function of the classifier is cubic given as  $\kappa(x_i, x_j)$

$$\kappa(x_i, x_j) = (x_i^T x_j)^3$$

It can be inferred that Cubic SVM presents a higher accuracy in recognizing all the four emotions correctly. Moreover, Cubic SVM is preferred due to its less computation time which was 10sec for a feature vector of dimension 12\*1 each for 100 samples. The SVM classifier is trained by varying the length of the feature vector. The testing process is executed for the buildings and non-buildings datasets separately.

## EXPERIMENTAL RESULTS

The results of the validated model is accuracy and plots, such as a scatter plot or the confusion matrix chart, reflect the validated model results. The data's are automatically train a selection of or all classifiers, compare validation results, and choose the best model that works for the classification problem.

In the scatter plot, view the classifier results. After train a classifier, the scatter plot switches from displaying the data to showing model predictions. There are using holdout or cross-validation, then these predictions are the predictions on the held-out observations. In other words, each prediction is obtained using a model that was trained without using the corresponding observation and use the controls on the right. Choose whether to plot model predictions or the data alone. Show or hide correct or incorrect results using the check boxes under Model predictions. Choose features to plot using the X and Y lists under Predictions. Visualize results by class by showing or hiding specific classes using the check boxes under Show. Change the stacking order of the plotted classes by selecting a class under Classes. X (column\_1) and Y (column\_2) is denoted as the length and width of the images. Original datasets are consists of data's to load the SVM and the prediction model to use the predicted the correct and incorrect date's.



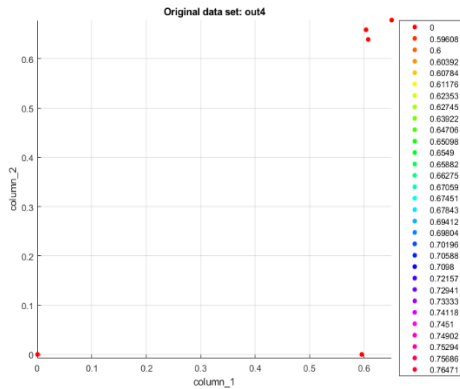


Figure: Original image of linear SVM

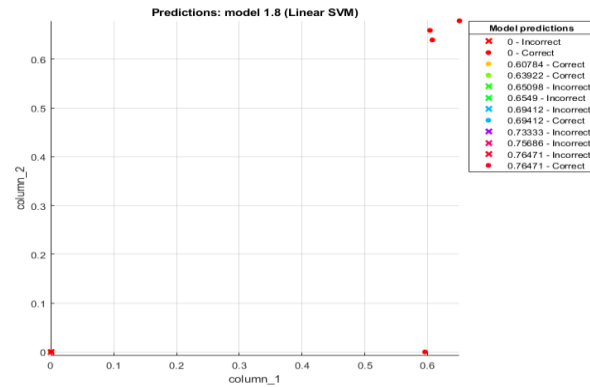


Figure: Prediction model of linear SVM

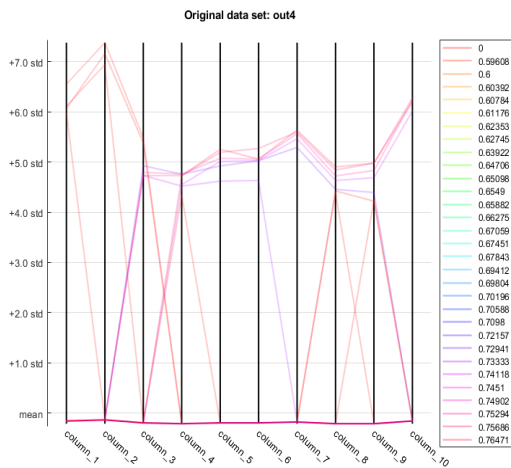


Figure: Tested original image of Linear SVM

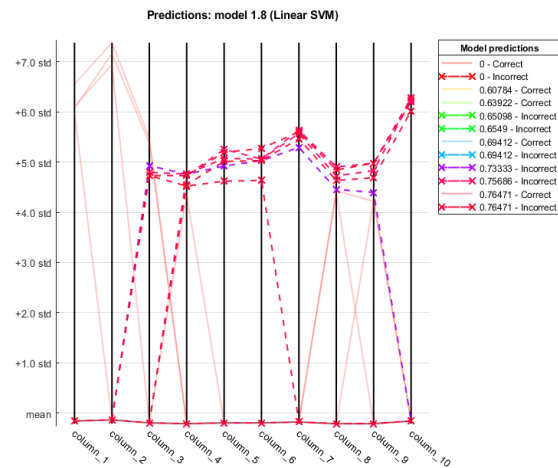


Figure: Tested Prediction of Linear SVM

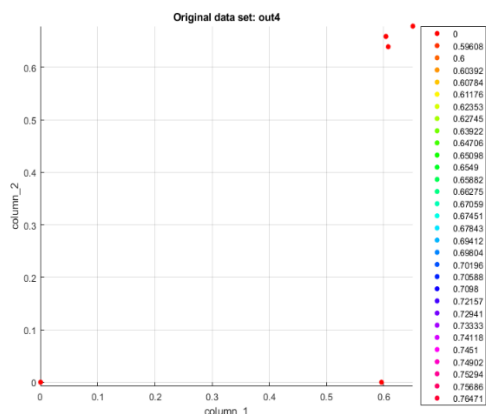


Figure: Original image of Cubic SVM

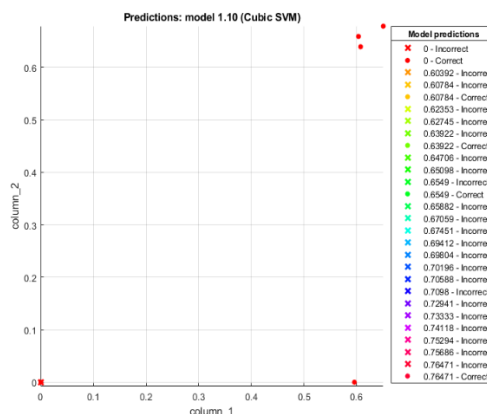


Figure: Prediction model of Cubic SVM

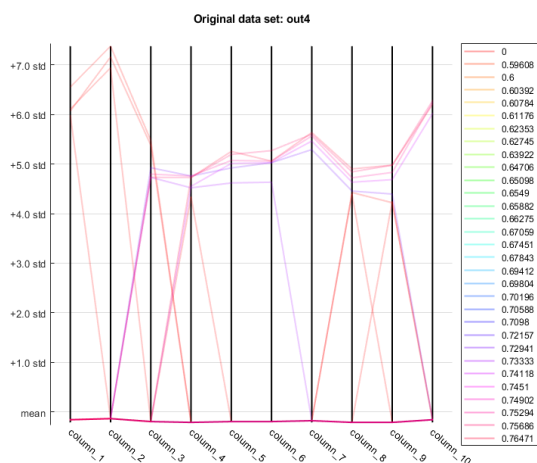


Figure: Tested original image of Cubic SVM

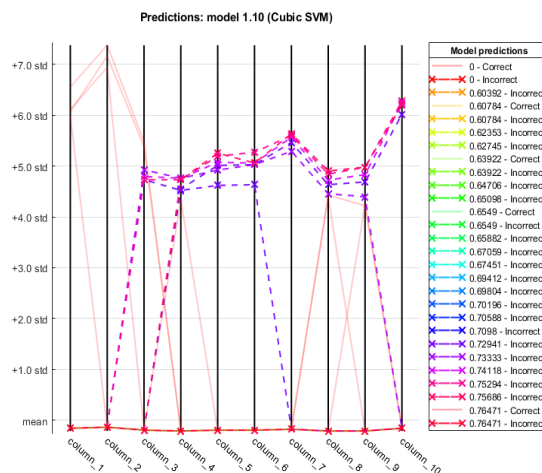


Figure: Tested Prediction of Cubic SVM

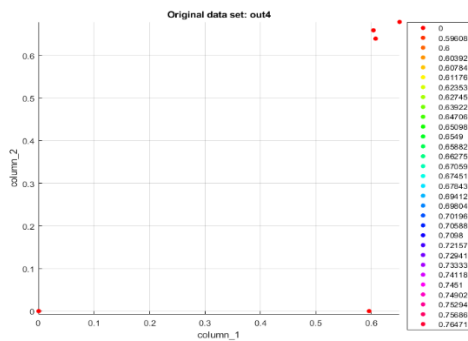


Figure: Original image of Medium Gaussian SVM

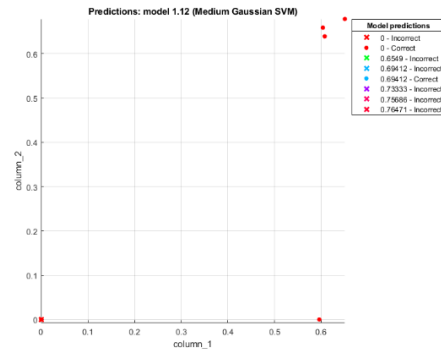


Figure: Prediction model of Medium Gaussian SVM

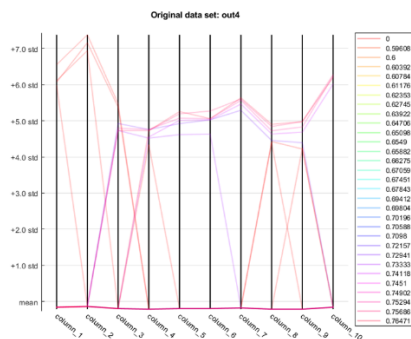


Figure: Tested original image of Medium Gaussian SVM

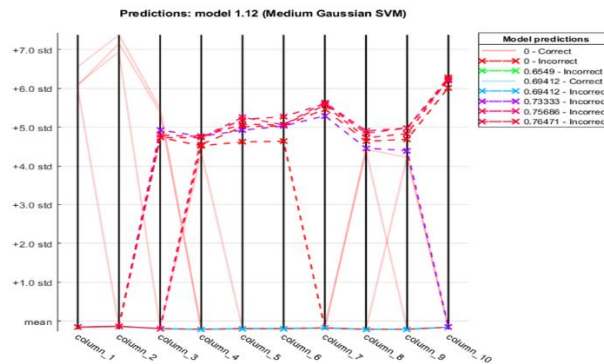


Figure: Tested Prediction of Cubic SVM Medium Gaussian SVM

## Confusion Matrix

Use the confusion matrix plot to understand how the currently selected classifier performed in each class. The confusion matrix helps you identify the areas where the classifier has performed poorly. When you open the plot, the rows show the true class, and the columns show the predicted class. If you are using holdout or cross-validation, then the confusion matrix is calculated using the predictions on the held-out observations. The diagonal cells show where the true class and predicted class match. If these cells are green, the classifier has performed well and classified observations of this true class correctly. The default view shows number of observations in each cell. To see how the classifier performed per class, under Plot, select the True Positive Rates, False Negative Rates option. The plot shows summaries per true class in the last two columns on the right.

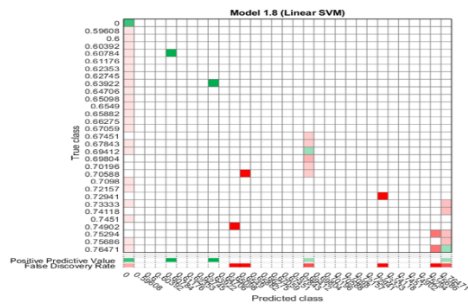


Figure:Confusion Matrix graph of linear SVM

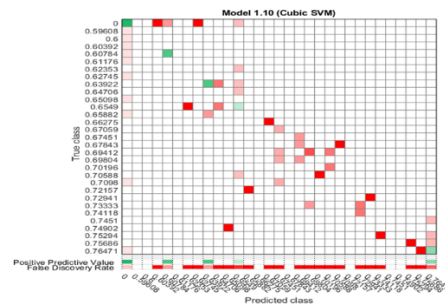


Figure:Confusion Matrix graph of Cubic SVM

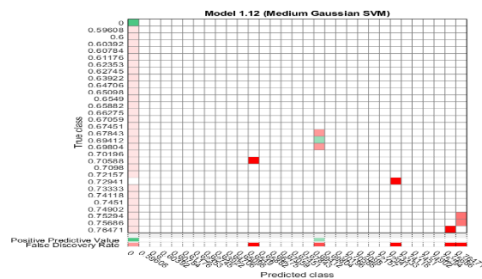


Figure:Confusion Matrix graph of Medium Gaussian SVM

## Receiver Operating Characteristic Curve

To view the receiver operating characteristic (ROC) curve after training a model, on the Classification Learner tab, in the Plots section, click ROC Curve. View the receiver operating characteristic (ROC) curve showing true and false positive rates. The ROC curve shows true positive rate versus false positive rate for the currently selected trained classifier. Can select different classes to plot.

The marker on the plot shows the performance of the currently selected classifier. The marker shows the values of the false positive rate (FPR) and the true positive rate (TPR) for the currently selected classifier. For example, a false positive rate (FPR) of 0.2 indicates that the current classifier assigns 20% of the observations incorrectly to the positive class. A true positive rate of 0.9 indicates that the current classifier assigns 90% of the observations correctly to the positive class.

A perfect result with no misclassified points is a right angle to the top left of the plot. A poor result that is no better than random is a line at 45 degrees. The Area under Curve number is a measure of the overall quality of the classifier. Larger Area under Curve values indicate better classifier performance. Compare classes and trained models to see if they perform differently in the ROC curve.

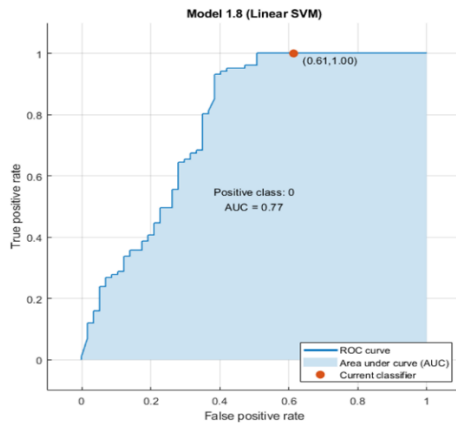


Figure: ROC curve of Linear SVM

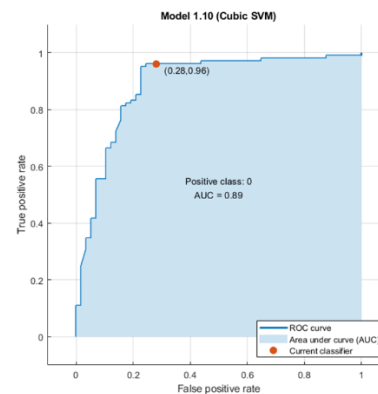


Figure: ROC curve of Cubic SVM

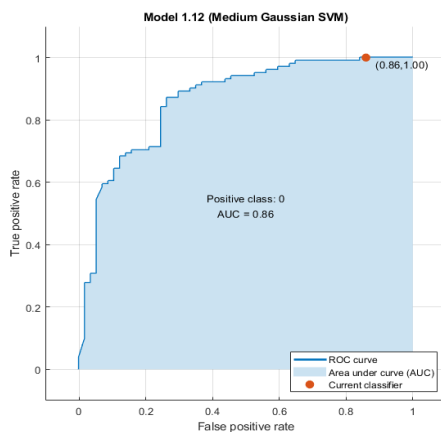


Figure: ROC curve of Medium Gaussian SVM

## Conclusion:

Overall, the three SVM classification approach was found very promising for Object-Based Image Analysis. It has been shown that it can produce comparable or even better results than for supervised classification. The computational efficiency of three SVM was great, with only a few minutes of runtime necessary for training. This was theoretically predicted but also, However, very large remote sensing datasets were tested. A very good feature of SVMs is that only a small training set is needed to provide very good results, because only the support vectors are of importance during training.

**Reference:**

- [1] Ahmadi H, Nusrath A. Vegetation change detection of Neka River in Iran by using remote-sensing and GIS. *Journal of geography and geology* 2010; 2 (1), 58-67.
- [2] Hacıhaliloglu I, Karta M. DCT and DWT based image compression in remote sensing images. In *proceeding IEEE conference on antennas and propagation society international symposium* 2004; 4, 3856-3858.
- [3] Karaburun A. Estimation of C factor for soil erosion modeling using NDVI in Buyukcekmece watershed. *Ozean journal of applied sciences* 2010; 3, 77-85.
- [4] V. Wan and W. M. Campbell, "Support vector machines for speaker verification and identification," in *Proc. IEEE Workshop Neural Networks for Signal Processing*, Sydney, Australia, Dec. 2000, pp. 775–784.
- [5] E. Osuna, R. Freund, and F. Girosi, "Training support vector machines: Application to face detection," in *Proc. Computer Vision and Pattern Recognition*, Puerto Rico, 1997, pp. 130–136.
- [6] J. Platt, "Fast training of support vector machines using sequential minimal optimization," in *Advances in Kernel Methods: Support Vector Learning*, B. Schölkopf, C. Burges, and A. J. Smola, Eds. Cambridge, MA: MIT Press, 1999, pp. 185–208.
- [7] J. Roehrig, T. Doi, A. Hasegawa, B. Hunt, J. Marshall, H. Romsdahl, A. Schneider, R. Sharbaugh, and W. Zhang, "Clinical results with R2 Imagechecker system," in *Digital Mammography*, N. Karssemeijer, M. Thijssen, J. Hendriks, and L. van Erning, Eds. Boston, MA: Kluwer Academic, 1998, pp. 395–400.
- [8] N. Karssemeijer, "A stochastic model for automated detection calcifications in digital mammograms," in *Proc. 12th Int. Conf. Information Medical Imaging*, Wye, U.K., July 1991, pp. 227–238.